GLM COMPREHENSIVE MODEL

FOR SOFT SCATTERING

Asher Gotsman and Uri Maor

Raymond and Beverly Sackler Faculty of Exact Science

Tel Aviv University, Tel Aviv, 69978, Israel

DEDICATED TO THE MEMORY OF MYRON BANDER

INTRODUCTION

Consider 3 paradoxes, dating back to the ISR epoch. They are resolved by unitarity screenings.

1) Whereas non screened σ_{tot} grows like s^{Δ}, σ_{el} grows faster, like $s^{2\Delta}$ (up to log corrections). With no screening, σ_{el} will, eventually, be larger than σ_{tot}.

2) Elastic and diffractive scatterings are seemingly similar. However, the energy dependence of the diffractive cross sections is significantly more moderate than that of σ_{el}.

3) The elastic amplitude is central in impact parameter b, peaking at b=0. The diffractive amplitudes are peripheral peaking at large b, which gets larger with energy.

As we shall see, models confined only to elastic scattering do not incorporate the full extent of unitarity screenings. Incorporating diffraction, is essential to a proper estimate of soft scatterings.

S-CHANNEL UNITARITY

The simplest s-channel unitarity bound on $a_{el}(s,b)$ is obtained from a diagonal re-scattering matrix, where repeated elastic re-scatterings secure s-channel unitarity. $2Ima_{el}(s,b) = |a_{el}(s,b)|^2 + G^{in}(s,b)$. **Its general solution is**

$$a_{el}(s,b) = i\left(1 - e^{-\Omega(s,b)/2}\right), \quad G^{in}(s,b) = 1 - e^{-\Omega(s,b)}. \quad \Omega \text{ is arbitrary.}$$

The output s-unitarity bound is $|\ a_{el}(s,b)\ | \leq 2$**, leading to very large total and elastic LHC cross sections, which are not supported by TOTEM recent data.**

In a Glauber type eikonal approximation, the input opacity $\Omega(s,b)$ is real. It equals to the imaginary part of the input Born term, a $I\!P$ exchange in our context. The output $a_{el}(s,b)$ is imaginary.

The consequent bound is $|\ a_{el}(s,b)\ | \leq 1$, **which is the black disc bound.**

In a single channel eikonal model, the screened cross sections are:

$$\sigma_{tot} = 2\int d^2b\left(1 - e^{-\Omega(s,b)/2}\right), \qquad \sigma_{el} = \int d^2b\left(1 - e^{-\Omega(s,b)/2}\right)^2, \qquad \sigma_{inel} = \int d^2b\left(1 - e^{-\Omega(s,b)}\right).$$

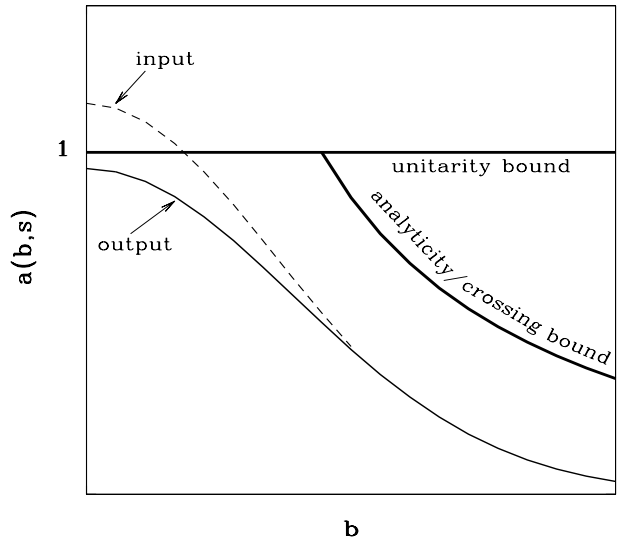

An illustration of the effects implied by unitarity screenings are shown in the figure above. It shows the s-channel black bound of unity, and the bound implied by analyticity/crossing symmetry on the expanding b-amplitude.

Imposing these limits leads to the Froissart-Martin bound

$$\sigma_{tot} \leq Cln^2(s/s_0), \quad s_0 = 1GeV^2, \quad C \propto 1/2m_\pi^2 \simeq 30mb.$$

C is far too large to be relevant in the analysis of TeV-scale data.

Coupled to Froissart-Martin is MacDowell-Martin bound: $\frac{\sigma_{tot}}{B_{el}} \leq 18\,\pi\,\frac{\sigma_{el}}{\sigma_{tot}}$.

Note that the Froissart limit controls the asymptotic behavior of the unitarity cross section bound, NOT the behavior of the elastic scattering cross section as such, which can have an arbitrary functional behavior as long as it is below saturation.

In t-space, σ_{tot} is proportional to a single point, $d\sigma_{el}/dt(t=0)$ (optical theorem).

As we saw, σ_{tot} in b-space is obtained from a b^2 integration over $2(1-e^{-\frac{1}{2}\Omega(s,b)})$.

Saturation in b-space is, thus, a differential feature, attained initially at b=0 and then expands very slowly with energy.

Consequently, a black core is a product of partial saturation, different from a complete saturation in which $a_{el}(s,b)$ is saturated at all b.

In a single channel model, $\sigma_{el} \leq \frac{1}{2}\sigma_{tot}$ and $\sigma_{inel} \geq \frac{1}{2}\sigma_{tot}$. At saturation, regardless of the energy at which it is attained, $\sigma_{el} = \sigma_{inel} = \frac{1}{2}\sigma_{tot}$.

Introducing diffraction, will significantly change the features of unitarity screenings. However, the saturation signatures remain valid.

POMERON MODEL

Translating the concepts presented into a viable phenomenology requires a specification of $\Omega(s,b)$, for which Regge theory is a powerful tool. Pomeron ($I\!P$) exchange is the leading term in the Regge hierarchy.

The growing total and elastic cross sections in the ISR-SPPS range are well reproduced by the non screened single channel DL $I\!P$ model in which:

$$\alpha_{I\!P}(t) = 1 + \Delta_{I\!P} + \alpha'_{I\!P} t, \qquad \Delta_{I\!P} = 0.08, \qquad \alpha'_{I\!P} = 0.25 GeV^{-2}.$$

$\Delta_{I\!P}$ determines the energy dependence, and $\alpha'_{I\!P}$ the forward slopes.

Regardless of DL remarkable success at lower energies, they under estimate the TEVATRON and LHC cross sections. This is traced to DL neglect of diffraction and unitarity screenings initiated by s and t dynamics.

Updated Pomeron models analyze elastic and diffractive channels utilizing s and t unitarity screenings.

GOOD-WALKER DECOMPOSITION

Consider a system of two orthonormal states, a hadron Ψ_h and a diffractive state Ψ_D. Ψ_D replaces the continuous diffractive Fock states. Good-Walker (GW) noted that Ψ_h and Ψ_D do not diagonalize the 2x2 interaction matrix T. Let Ψ_1 and Ψ_2 be eigen states of T.

$$\Psi_h = \alpha\Psi_1 + \beta\Psi_2, \quad \Psi_D = -\beta\Psi_1 + \alpha\Psi_2, \quad \alpha^2 + \beta^2 = 1.$$

The eigen states initiate 4 $A_{i,k}$ elastic GW amplitudes $(\psi_i + \psi_k \to \psi_i + \psi_k)$. i,k=1,2. For initial $p(\bar{p}) - p$ we have $A_{1,2} = A_{2,1}$. I shall follow the GLM definition, in which the mass distribution associated with Ψ_D is not defined.

The elastic, SD and DD amplitudes in a 2 channel GW model are:

$$a_{el}(s,b) = i\{\alpha^4 A_{1,1} + 2\alpha^2\beta^2 A_{1,2} + \beta^4 A_{2,2}\},$$

$$a_{sd}(s,b) = i\alpha\beta\{-\alpha^2 A_{1,1} + (\alpha^2 - \beta^2)A_{1,2} + \beta^2 A_{2,2}\},$$

$$a_{dd}(s,b) = i\alpha^2\beta^2\{A_{1,1} - 2A_{1,2} + A_{2,2}\},$$

$$A_{i,k}(s,b) = \left(1 - e^{\frac{1}{2}\Omega_{i,k}(s,b)}\right) \leq 1.$$

GW mechanism changes the structure of s-unitarity below saturation.

- **In the GW sector we obtain the Pumplin bound:** $\sigma_{el} + \sigma_{diff}^{GW} \leq \frac{1}{2}\sigma_{tot}$**.** σ_{diff}^{GW} **is the sum of the GW soft diffractive cross sections.**
- **Below saturation,** $\sigma_{el} \leq \frac{1}{2}\sigma_{tot} - \sigma_{diff}^{GW}$ **and** $\sigma_{inel} \geq \frac{1}{2}\sigma_{tot} + \sigma_{diff}^{GW}$**.**
- $a_{el}(s,b) = 1$**, when and only when,** $A_{1,1}(s,b) = A_{1,2}(s,b) = A_{2,2}(s,b) = 1$**.**
- **When** $a_{el}(s,b) = 1$**, all diffractive amplitudes at the same (s,b) vanish.**
- **As we shall see, there is a distinction between GW and non GW diffraction. Regardless, GW saturation signatures are valid also in the non GW sector.**
- **As we saw, the saturation signature,** $\sigma_{el} = \sigma_{inel} = \frac{1}{2}\sigma_{tot}$**, in a multi channel calculation is coupled to** $\sigma_{diff} = 0$**. Consequently, prior to saturation the diffractive cross sections stop growing and start to decrease with energy. This is a clear signature preceding saturation.**

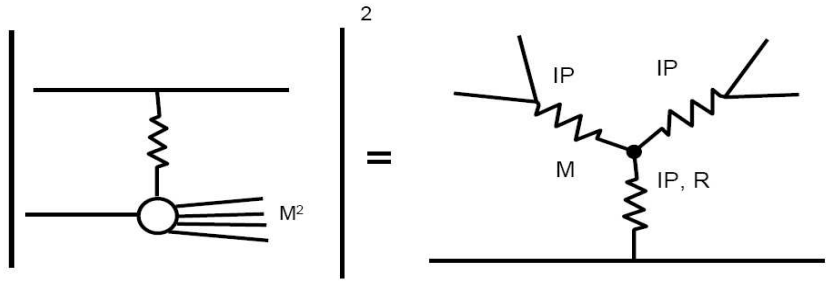

CROSSED CHANNELED UNITARITY

Mueller(1971) applied 3 body unitarity to equate the cross section of $a + b \to M_{sd}^2 + b$ to the triple Regge diagram $a + b + \bar{b} \to a + b + \bar{b}$. shown above.

The signature of this presentation is a triple vertex with a leading $3\mathbb{P}$ term.

The $3\mathbb{P}$ approximation is valid when, $\frac{m_p^2}{M_{sd}^2} << 1$ and $\frac{M_{sd}^2}{s} << 1$.

The leading energy/mass dependences are $\frac{d\sigma^{3\mathbb{P}}}{dt\, dM_{sd}^2} \propto s^{2\Delta_{\mathbb{P}}} \left(\frac{1}{M_{sd}^2}\right)^{1+\Delta_{\mathbb{P}}}$.

Mueller's $3\mathbb{P}$ approximation for non GW diffraction is the lowest order of t-channel multi $\mathbb{P}$ interactions, which induce compatibility with t-channel unitarity.

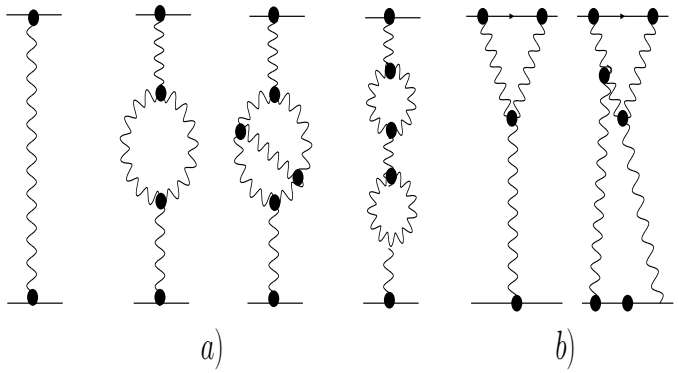

Recall that unitarity screening of GW ("low mass") diffraction is carried out explicitly by eikonalization, while the screening of non GW ("high mass") diffraction is carried out by the survival probability (to be discussed).

The figure above shows the $I\!P$ Green function. Multi $I\!P$ interactions are summed differently in the various $I\!P$ models.

Note the analogy with QED renormalization:

a) Enhanced diagrams, present the renormalization of the propagator.

b) Semi enhanced diagrams, present the p$I\!P$p vertex renormalization.

SURVIVAL PROBABILITY

The experimental signature of a $I\!P$ exchanged reaction is a large rapidity gap (LRG), devoid of hadrons in the $\eta - \phi$ Lego plot, $\eta = -ln(tan\frac{\theta}{2})$.

S^2, the LRG survival probability, is a unitarity induced suppression factor of non GW diffraction, soft or hard: $S^2 = \sigma_{diff}^{screened}/\sigma_{diff}^{nonscreened}$.

It is the probability that the LRG signature will not be filled by debris (partons and/or hadrons) originating from either the s-channel re-scatterings of the spectator partons, or by the t-channel multi $I\!P$ interactions.

Denote the gap survival factor initiated by s-channel eikonalization S^2_{eik}, and the one initiated by t-channel multi $I\!P$ interactions, S^2_{enh}.

The eikonal re-scatterings of the incoming projectiles are summed over (i,k).

S^2 is obtained from a convolution of S^2_{eik} and S^2_{enh}.

A simpler, reasonable approximation, is $S^2 = S^2_{eik} \cdot S^2_{enh}$.

THE PARTONIC POMERON

Current $I\!P$ models differ in details, but have in common a relatively large adjusted input $\Delta_{I\!P}$ and a diminishing $\alpha'_{I\!P}$.

The exceedingly small fitted $\alpha'_{I\!P}$ implies a partonic description of the $I\!P$ which leads to a pQCD interpretation.

The microscopic sub structure of the $I\!P$ is obtained from Gribov's partonic interpretation of Regge theory, in which the slope of the $I\!P$ trajectory is related to the mean transverse momentum of the partonic dipoles constructing the Pomeron and, consequently, the running QCD coupling:

$$\alpha'_{I\!P} \propto 1/ < p_t >^2, \qquad \alpha_S \propto \pi/ln\left(< p_t^2 > /\Lambda^2_{QCD}\right) << 1.$$

We obtain a single $I\!P$ with hardness depending on external conditions.

This is a non trivial relation as the soft $I\!P$ is a simple moving pole in J-plane, while, the BFKL hard $I\!P$ is a branch cut approximated, though, as a simple pole with $\Delta_{I\!P} = 0.2 - 0.3$, $\alpha'_{I\!P} = 0$.

GLM and KMR models are rooted in Gribov's partonic $\mathbb{P}$ theory with a hard pQCD $\mathbb{P}$ input. It is softened by unitarity screening (GLM), or the decrease of its partons' transverse momentum (KMR).

An added bonus of the GLM formalism is its compatibility with N=4 SYM.

GLM and KMR models have a bound of validity, at 60(GLM) and 100(KMR) TeV, implied by their approximations. Consequently, as attractive as updated $\mathbb{P}$ models are, we can not utilize them above 100 TeV.

To this end, the only available models are single channel, most of which have a logarithmic parametrization input. The main deficiency of such models is that while they provide a good reproduction of the available total and elastic data, their predictions at higher energies are questionable since diffractive channels and t-channel screening are not included.

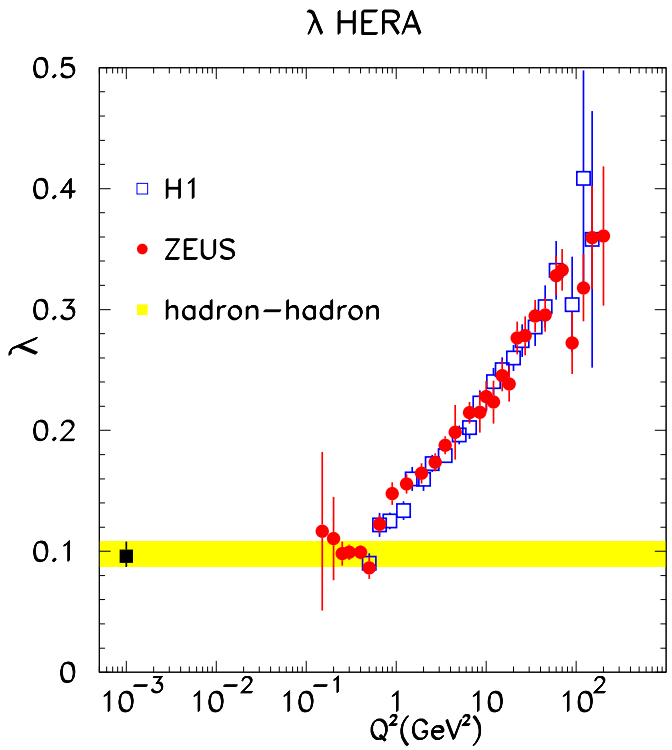

The single $\mathbb{P}$ picture suggested by the updated $\mathbb{P}$ models implies a smooth transition from the input hard $\mathbb{P}$ to a soft $\mathbb{P}$. This picture is supported by the the HERA dependence of $\lambda = \Delta_{\mathbb{P}}$ on Q^2 shown in the figure above.

MODEL PREDICTIONS

Updated Pomeron models depend on the adjustment of many free parameters while the data base they are designed to reproduce is relatively small. This problem has been addressed differently in each of the relevant models.

In the following I shall present the output of the GLM model and compare it with the available data in the ISR-AUGER energy range. I shall, also, present the main outputs of 3 leading models in the TeV-scale.

- **GLM and KMR, which are $I\!P$ models quite similar conceptually, but different in their approximations and statistical procedures.**
- **Block and Halzen (BH), which is a representative single channel model based on a logarithmic parametrization, addressing only the total and elastic cross sections.**

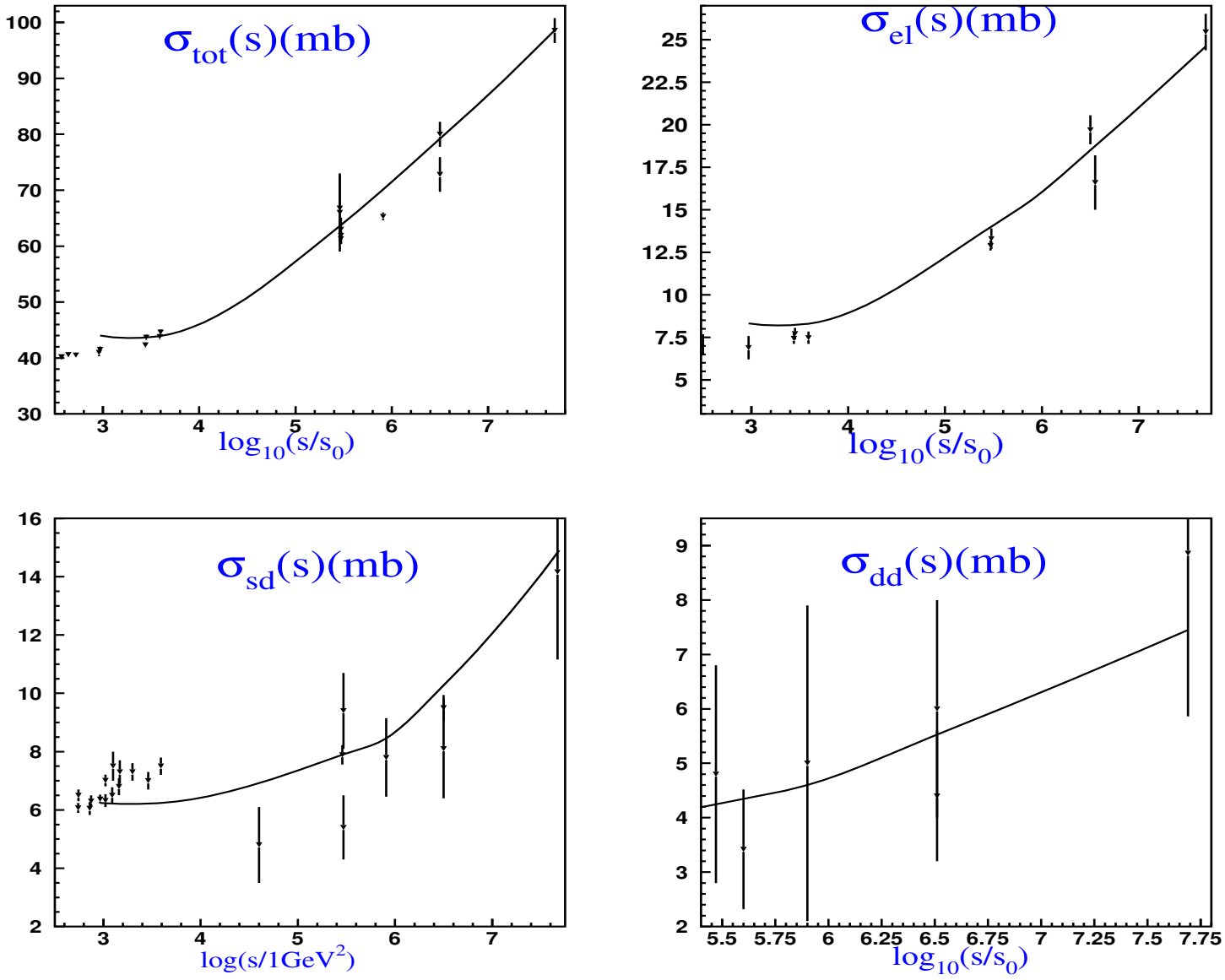

FIG. 1: A) GLM CROSS SECTIONS

	$7\,TeV$		$14\,TeV$		$57\,TeV$	$100\,TeV$	
	GLM	KMR	GLM	KMR	GLM	GLM	KMR
σ_{tot}	98.6	97.4	109.0	107.5	130.0	134.0	138.8
σ_{el}	24.6	23.8	27.9	27.2	34.8	37.5	38.1
σ_{sd}^{GW}	10.7	7.3	11.5	8.1	13.0	13.6	10.4
σ_{sd}	14.88		17.31		21.68		
σ_{dd}^{GW}	6.21	0.9	6.79	1.1	7.95	8.39	1.6
σ_{dd}	7.45		8.38		18.14		
$\frac{\sigma_{el}+\sigma_{diff}^{GW}}{\sigma_{tot}}$	0.42	0.33	0.42	0.34	0.43	0.43	0.36

B) $I\!P$ MODELS PREDICTED CROSS SECTIONS IN THE TEV-SCALE

GLM and KMR σ_{tot}, σ_{el}, σ_{sd}, σ_{dd} at 7-100TeV are presented above.

GLM and KMR σ_{tot} and σ_{el} are compatible.

KMR confine their diffractive predictions to the GW sector.

GLM GW σ_{sd} and σ_{dd} are larger than KMR.

In both models, the GW components are compatible with the Pumplin bound.

	$7\,TeV$			$14\,TeV$			$57\,TeV$		$100\,TeV$		
	GLM	KMR	BH	GLM	KMR	BH	GLM	BH	GLM	KMR	BH
σ_{tot}	98.6	97.4	95.4	109.0	107.5	107.3	130.0	134.8	139.0	138.8	147.1
σ_{inel}	74.0	73.6	69.0	81.1	80.3	76.3	95.2	92.9	101.5	100.7	100.0
$\frac{\sigma_{inel}}{\sigma_{tot}}$	0.75	0.76	0.72	0.74	0.75	0.71	0.73	0.70	0.73	0.73	0.68

C) UNITARITY SATURATION

The possibility of unitarity saturation, at increasingly high energy, is coupled to 2 signatures: **i)** $\frac{\sigma_{inel}}{\sigma_{tot}} = \frac{\sigma_{el}}{\sigma_{tot}} = 0.5$, *and* **ii)** $\sigma_{diff} = 0$.

Checking the available experimental cross section data at the TeV-scale, we get: $\sigma_{inel}/\sigma_{tot} = 0.75(CDF), 0.75(TOTEM), 0.69(AUGER)$.

These results are supported by the Table above, which compares the outputs of GLM, KMR and BH at 7-100 TeV.

The 3 models have compatible $\frac{\sigma_{inel}}{\sigma_{tot}}$ outputs in the TeV-scale which are significantly larger than 0.5.

The BH model can be applied at arbitrary high energies. The prediction of BH at the Planck-scale ($\mathbf{1.22}\cdot 10^{16} TeV$) is, $\sigma_{inel}/\sigma_{tot} = 1131mb/2067mb = 0.55$, which is below a_{el} saturation.

The persistent growth of the diffractive cross sections predictions indicates that saturation will be attained (if at all) well above the TeV-scale.

Note that:

GLM 100 TeV predictions are somewhat above the model validity bound.

The analysis of diffraction, is hindered by different choices of signatures and bounds!

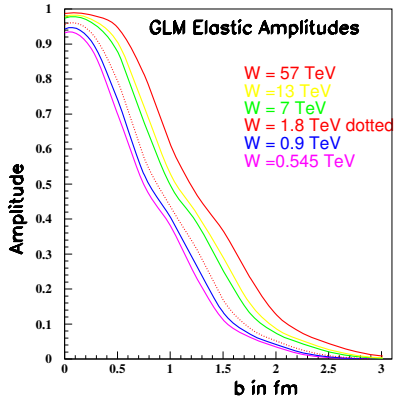

Our observation that unitarity saturation of the elastic p-p amplitude can not be attained at realistic energies, does not infer on the probable possibility of a black core in the p-p amplitude. This option is model dependent. Indeed, the $I\!P$ models differ in their estimate of this possible phenomenon.

In the figure above we show the GLM predicted elastic b-amplitudes. As seen, the increase of $a_{el}(b=0,s)$ is very slow, and we expect the p-p elastic amplitude to develop a black core at $W \geq 60TeV$.